Engineering impurity Bell states through coupling with a quantum bath

Tran Duong Anh-Tai,[1,*] Thomás Fogarty,[1,†] Sergi de María-García,[2] Thomas Busch,[1] and Miguel A. García-March[2,‡]

[1]*Quantum Systems Unit, OIST Graduate University, Onna, Okinawa 904-0495, Japan*

[2]*Instituto Universitario de Matemática Pura y Aplicada, Universitat Politècnica de València, E-46022 València, Spain*

(Received 19 June 2024; accepted 9 September 2024; published 16 October 2024)

We theoretically demonstrate the feasibility of creating Bell states in multicomponent ultracold atomic gases by solely using the ability to control the interparticle interactions via Feshbach resonances. For this we consider two distinguishable impurities immersed in an atomic background cloud of a few bosons, with the entire system being confined in a one-dimensional harmonic trap. By analyzing the numerically obtained ground states we demonstrate that the two impurities can form spatially entangled bipolaron states due to mediated interactions from the bosonic bath. Our analysis is based on calculating the correlations between the two impurities in a two-mode basis, which is experimentally accessible by measuring the particle positions in the left or right sides of the trap. While interspecies interactions are crucial in order to create the strongly entangled impurity states, they can also inhibit correlations depending on the ordering of the impurities and three-body impurity-bath correlations. We show how these drawbacks can be mitigated by manipulating the properties of the bath, namely its size, mass, and intraspecies interactions, allowing one to create impurity Bell states over a wide range of impurity-impurity interactions.

DOI: 10.1103/PhysRevResearch.6.043042

I. INTRODUCTION

Great advancements in the development of techniques to experimentally realize, control, and measure various quantum systems made from single or few particles are currently fueling a *second quantum revolution* [1–3]. The resulting quantum technologies rely crucially on the possibility to create and maintain entanglement in these systems [4], and one of the most useful states is the maximally entangled Bell state [5]. In this state two systems, A and B, are maximally correlated and each of them holds all possible information about some observable from the other. Therefore creating and controlling correlated quantum states, especially the Bell states, in experimentally accessible systems is of importance and will be beneficial for advancing fundamental science and quantum technologies.

Cold atom systems have proven over the last two decades that they are very suitable systems to control and study single- and few-particle states [6,7]. In particular, the long-standing problem of impurities coupled to an environment has been of immense interest ever since the availability of experimental systems in recent years [8–16]. Cold atomic settings allow one to access different parameter regimes and therefore simulate a wider range of interesting phenomena, which are often difficult to study with the same amount of control in condensed matter setups. Impurity physics can be conveniently discussed in terms of polarons, which are quasiparticles that are dressed by the excitations of the surrounding medium [17]. One of the most fascinating aspects of polarons is the induced interactions between them mediated by the quantum many-body environment in which they are immersed. For example, two uncorrelated impurities which are coupled to the same Bose-Einstein condensate (BEC) can form a bound state (known as a bipolaron) due to the bath-mediated attractive interactions [18–23]. One of the theoretical frameworks that can successfully describe impurities in ultracold gases is the mapping of the BEC-impurity problem to the Fröhlich polaron Hamiltonian which describes electron-phonon interactions in condensed matter physics [24–27]. For a more accurate description of impurity physics that takes the exact effects of all interactions into account, one has to go beyond the Fröhlich model [28]. While in weakly interacting gases the Gross-Pitaevskii theory (see Refs. [29–31] and references therein) or the quantum Brownian motion framework [16,19,32–34] can be used to describe the ground state of the BEC-impurities system, in the strongly interacting regime where particle-particle correlations are prominent, the system has to be solved from first principles. It is also important to note that two recent works have shown that the impurity-bath correlations play a crucial role and result in the suppression of impurity self-localization [35,36], which is not captured by the mean-field approach. This demonstrates that a full quantum treatment of the BEC-impurity problem is necessary, although it is not a trivial task to

*Contact author: tai.tran@oist.jp
†Contact author: thomas.fogarty@oist.jp
‡Contact author: garciamarch@mat.upv.es

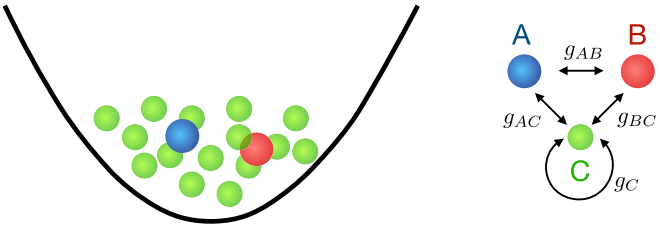

FIG. 1. Schematic of the model. The N_C bosons of mass m_C form an interacting bath that two distinguishable impurities, A and B, of the mass m are immersed in. The entire system is confined in a one-dimensional harmonic trap and all particles interact with all others.

accurately solve many-body systems with different intraspecies and interspecies interactions in the continuum due to the exponential growth of Hilbert space. However, in one dimension some exact numerical tools are available and recently the nonclassical correlations in stationary and out-of-equilibrium situations have been explored using exact diagonalization methods [37,38], or the multilayer multiconfiguration time-dependent Hartree method for mixtures of identical particles [39–42]. Since the impurities can become entangled with each other due to bath induced interactions, we suggest that it is possible to control correlations between impurities by engineering the interaction with the quantum bath alone.

In the following we propose a method to engineer strongly correlated atomic states in ultracold, one-dimensional (1D) interacting atomic systems using the ability to control the interparticle and intraparticle interactions via Feshbach resonances. More specifically, we consider two distinguishable impurities immersed into a third larger background component composed of a well-defined number of bosons confined in a harmonic trap (see Fig. 1). We systematically investigate the ground state of such an interacting three-component mixture by employing the improved exact diagonalization scheme [43] to exactly solve the many-body Schrödinger equation describing our system (see also the Appendix). As a main result of the present paper we demonstrate how to fully engineer nonclassical correlations between two distinguishable impurities by tuning the impurity-impurity and bath intraspecies interactions while the impurity-bath coupling is always repulsive. We find that for strong repulsive interactions between the impurities and the bath, the impurities phase separate to the trap edges, while the bath is localized in the trap center. This allows one to describe the impurities in a discrete spatial basis of the left and right halves of the trap and facilitates the measurement of spatial entanglement and correlation between the impurities [44]. Our results show that the impurities can form maximally entangled Bell states due to the competition between the different interaction terms; however, the correlations created between the impurities and the bath can impair Bell state formation. This depends on whether the impurities are bunched or antibunched, which we explain through the analysis of tripartite correlation functions. Finally, we show how the properties of the bath can be tuned to reduce these higher order correlations, allowing one to create strongly entangled impurity states via bath mediated interactions.

This paper is structured as follows: Sec. II presents the model and quantities of interest, while Sec. III discusses how impurity-impurity correlations can be induced by the bosonic bath. In Sec. IV we discuss how to significantly enhance the impurity-impurity correlations by engineering the bath, and the conclusions and outlook are drawn in Sec. V.

II. MODEL AND QUANTITIES OF INTEREST

The three-component mixture of interacting ultracold bosons we consider consists of two distinguishable atoms of species A and B, which are immersed in a background cloud of N_C atoms of species C. The atoms A and B are assumed to have the same mass $m_A = m_B = m$, while the C atoms have the mass m_C. Since at ultracold temperatures the s-wave scattering process is dominant, the interaction between any two particles can be described by a contact interaction potential [45], and we assume that the strengths of all intracomponent and intercomponent scattering lengths can be independently adjusted using Feshbach [46] or induced-confinement resonances [47]. For numerical simplicity and experimental relevance, we also assume that all particles are trapped in a one-dimensional parabolic potential with frequency ω, and hence, the Hamiltonian of this system can be written as $\hat{\mathcal{H}} = \hat{\mathcal{H}}_\sigma + \hat{\mathcal{W}}_C + \hat{\mathcal{W}}_{\sigma\delta}$ where

$$\begin{aligned}
\hat{\mathcal{H}}_\sigma &= \sum_\sigma \sum_{i=1}^{N_\sigma} \left[-\frac{\hbar^2}{2m_\sigma} \frac{d^2}{dx_{\sigma,i}^2} + \frac{1}{2} m_\sigma \omega^2 x_{\sigma,i}^2 \right], \\
\hat{\mathcal{W}}_C &= \frac{1}{2} g_C \sum_{i<j}^{N_C} \delta(x_{C,i} - x_{C,j}), \\
\hat{\mathcal{W}}_{\sigma\delta} &= g_{\sigma\delta} \sum_{i=1}^{N_\sigma} \sum_{j=1}^{N_\delta} \delta(x_{\sigma,i} - x_{\delta,j}).
\end{aligned} \tag{1}$$

Since we consider only one atom each of species A and B ($N_A = N_B = 1$) our setting resembles a two-impurity problem. We therefore term the component C as a bosonic bath, within which the intraspecies interactions are characterized by g_C. The interspecies interactions are denoted by $g_{\sigma\delta}$ with $\sigma \neq \delta \in \{A, B, C\}$ and describe the impurity-impurity interaction g_{AB} and the impurity-bath interactions g_{AC} and g_{BC}. In (quasi-)one-dimensional systems, the contact interaction potential can be modeled by a bare δ function [48]. For the sake of simplicity, we rescale all lengths, energies, and coupling strengths by harmonic oscillator units given by $\sqrt{\hbar/(m\omega)}$, $\hbar\omega$, and $\sqrt{\hbar^3\omega/m}$, respectively.

Three-component ultracold quantum gases have been experimentally created [49,50] and their properties can vary widely due to the large parameter space the different interaction strengths span. To make the problem tractable, we therefore restrict the interaction strengths between the immersed atoms and the bath to be equal and repulsive, $g_{AC} = g_{BC} > 0$, while the interaction between the impurities, g_{AB}, and the intraspecies interaction g_C can be either attractive or repulsive. We also fix the maximum number of C-species bosons to be $N_C = 10$ as this is the limit of our numerical simulations. However, as we will show this bath size is more than sufficient to explore the role of bath mediated interactions and correlations, and is in a similar parameter regime as previous studies [42].

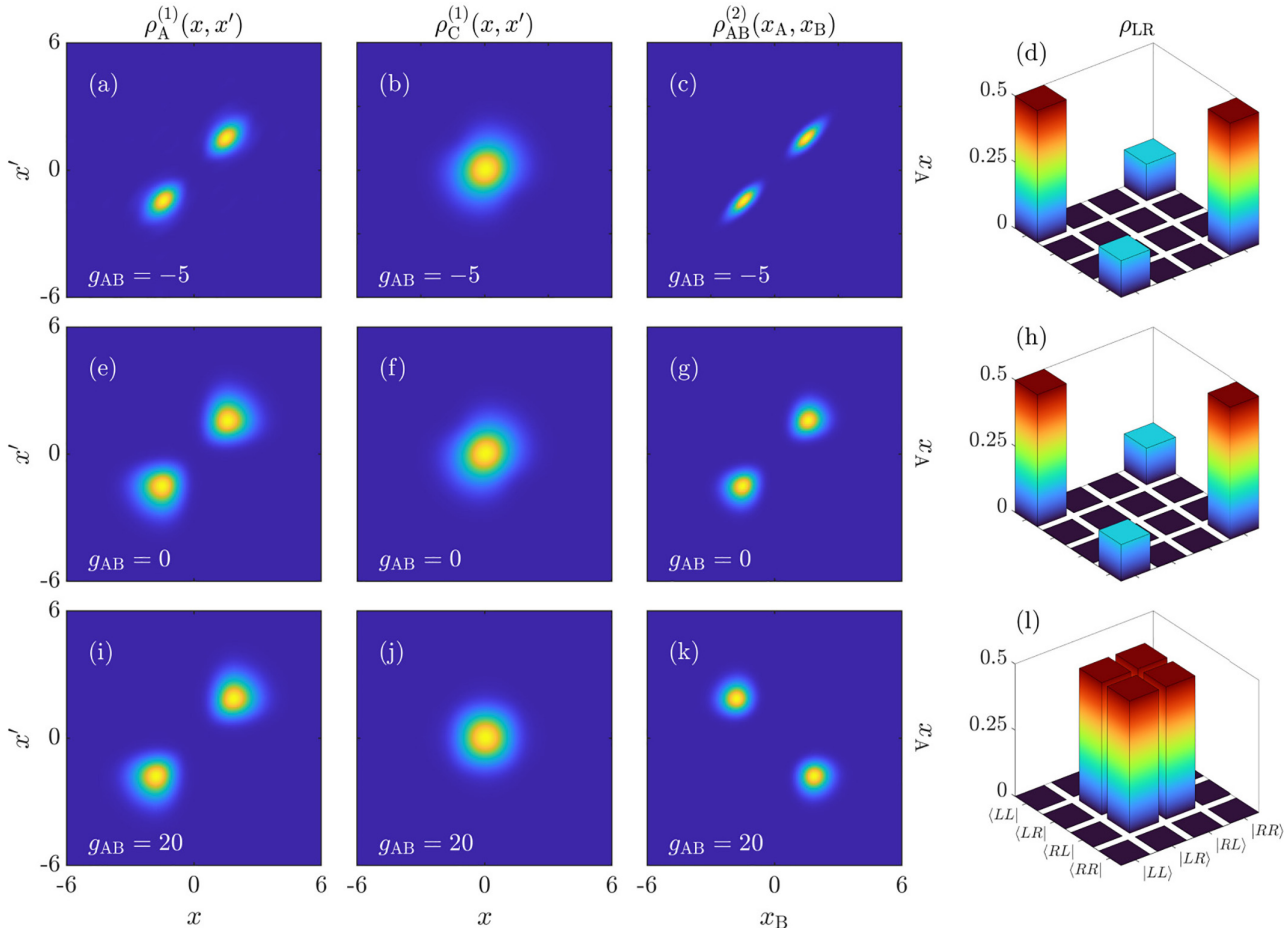

FIG. 2. The four columns show the OBDM $\rho_A^{(1)}(x,x')$, the OBDM $\rho_C^{(1)}(x,x')$, the diagonal TBDM $\rho_{AB}^{(2)}(x_A,x_B)=\rho_{AB}^{(2)}(x_A,x_B,x_A,x_B)$, and the reduced density matrix $\rho_{\rm LR}$ of the many-body ground state of the system for $N_C=10$. The different rows correspond to different impurity-impurity coupling strengths, $g_{AB}=-5$ (upper row), $g_{AB}=0$ (middle row), and $g_{AB}=20$ (lower row). In all panels, the bosonic bath is noninteracting, $g_C=0$, while the impurity-bath coupling strengths are kept fixed, $g_{AC}=g_{BC}=5$, and the masses are identical, $m_C/m=1$. Note that all density matrices are normalized to unity.

To determine the ground state $|{\rm GS}\rangle$ and explore the quantum properties of the three-component system we will solve Eqs. (1) numerically exactly using the improved diagonalization method [43]. This numerical tool allows us to explicitly access the quantum correlations via the one-body reduced density matrix (OBDM) and the two-body reduced density matrix (TBDM) defined as

$$\rho_\sigma^{(1)}(x_\sigma,x'_\sigma)=\langle\hat\Psi_\sigma^\dagger(x)\hat\Psi_\sigma(x')\rangle, \tag{2}$$

$$\rho_{\sigma\delta}^{(2)}(x_\sigma,x_\delta,x'_\sigma,x'_\delta)=\langle\hat\Psi_\sigma^\dagger(x_\sigma)\hat\Psi_\delta^\dagger(x_\delta)\hat\Psi_\sigma(x'_\sigma)\hat\Psi_\delta(x'_\delta)\rangle, \tag{3}$$

where $\hat\Psi_\sigma^{(\dagger)}(x)$ is the bosonic field operator annihilating (creating) a σ-type boson at the position x and averages are taken with respect to the many-body ground state, $|{\rm GS}\rangle$, of the Hamiltonian (1). To structure our results, we first fix some of the parameters by choosing the impurity-bath coupling as $g_{AC}=g_{BC}=5$ and considering the masses of all the particles to be identical, $m_C/m=1$. This allows us to focus on the following three representative cases for the impurity-impurity interaction: case I where $g_{AB}<0$, case II where $g_{AB}=0$, and case III where $g_{AB}>0$. In the two left columns of Fig. 2 we show the OBDMs of the A (the one for B is identical for symmetry reasons) and the C components. One can see that for all different impurity-impurity interactions the impurities localize towards the trap edges, while the particles of the bath are located in the center of the trap. The total system is therefore in a regime of phase separation due to the large impurity-bath interactions and the size of the bath. While this describes the spatial separation of the impurities, an analysis of the diagonal of the TBDM, $\rho_{AB}^{(2)}(x_A,x_B)$ (shown in the third column of Fig. 2), reveals that the joint probability of finding impurities A and B on either side of C is strongly dependent on the impurity-impurity interaction. Specifically, the impurities antibunch for repulsive interactions (case III $g_{AB}=20$) and bunch for attractive interactions (case I $g_{AB}=-5$). Bunching is also apparent for case II, when the impurity-impurity interaction is absent, as a bound state is formed due to induced attractive impurity-impurity interactions mediated by the C component. This distinctive bound state is known as the bipolaron [18,20–23]. The TBDM in Fig. 2(g) therefore suggests the combination of bath mediated attractive interactions and suitably large repulsive impurity-bath interactions allows one to create a superposition state of a bipolaron localized at each

side of the C component, and that this state has a large degree of spatial entanglement. We will explore this in more detail in the next section.

III. BATH INDUCED IMPURITY-IMPURITY CORRELATIONS

To quantify the entanglement between the impurities we first note that in all cases species C can be seen to play the role of a matter-wave barrier located in the center of the trap. This allows us to characterize the impurity states using a discrete spatial basis $|\mathrm{L}\rangle$ and $|\mathrm{R}\rangle$ that represents the left ($x < 0$) and right ($x > 0$) sides of the trap respectively, while we denote the centrally localized C particles by $|C\rangle$.

The precise state which the two impurities are in can then be determined by considering the reduced density matrix of the impurities ρ_{LR}, which is a positive semidefinite Hermitian operator whose elements are constructed by integrating the TBDM $\rho^{(2)}_{AB}(x_A, x_B, x'_A, x'_B)$ over the corresponding spatial regions, i.e., $|\mathrm{L}\rangle \in (-\infty, 0)$ and $|\mathrm{R}\rangle \in (0, +\infty)$. In Figs. 2(d), 2(h), and 2(l) we show the reduced density matrices for the three cases we consider. One can immediately note that Fig. 2(l) precisely exhibits the density matrix of the Bell state $|\Psi^+\rangle = (|\mathrm{LR}\rangle + |\mathrm{RL}\rangle)/\sqrt{2}$, which is a strong signature that the impurities are maximally entangled in case III. However, while in cases I and II the occupation of the diagonal elements $|\mathrm{LL}\rangle\langle\mathrm{LL}|$ and $|\mathrm{RR}\rangle\langle\mathrm{RR}|$ indicates that the impurities form tight bound states, the coherence terms $|\mathrm{LL}\rangle\langle\mathrm{RR}|$ and $|\mathrm{RR}\rangle\langle\mathrm{LL}|$ are significantly diminished. This implies that these states are not the maximally entangled $|\Phi^+\rangle = (|\mathrm{LL}\rangle + |\mathrm{RR}\rangle)/\sqrt{2}$ Bell states, and that some decoherence is being caused by the coupling to the C component. Therefore, correlations between the impurities and the matter-wave barrier have a considerable effect on impurity-impurity entanglement, which is substantially different from double-well potentials created by classical optical fields as used in most current ultracold atomic setups [44]. We do stress however, that the matter-wave barrier and the aforementioned induced interactions are essential for the creation of the bipolaron Bell state (case II), as classical fields alone are not sufficient to create this state.

To quantify the degree of entanglement of the state ρ_{LR} we calculate the concurrence

$$\mathcal{C} = \max(0, \sqrt{\lambda_1} - \sqrt{\lambda_2} - \sqrt{\lambda_3} - \sqrt{\lambda_4}) \tag{4}$$

where the λ_j are the ascending-order eigenvalues of $\rho_{\mathrm{LR}}(\sigma_y \otimes \sigma_y)\rho^*_{\mathrm{LR}}(\sigma_y \otimes \sigma_y)$ with σ_y being the Pauli y matrix. Furthermore we must consider the separability of the impurities from the C component. This can be quantified by the von Neumann entropy

$$S^{\mathrm{vN}}_{AB} = -\mathrm{Tr}[\rho_{AB}\log_2(\rho_{AB})], \tag{5}$$

where $\rho_{AB} = \mathrm{Tr}_C|\mathrm{GS}\rangle\langle\mathrm{GS}|$ is the reduced density matrix of the impurities after tracing out the bath. The condition for the impurities to be separable from the bath is therefore $S^{\mathrm{vN}}_{AB} = 0$.

In Figs. 3(a) and 3(b) we show the concurrence and the von Neumann entropy as a function of the impurity-impurity interaction g_{AB} for $m_C = m$ (black lines). In the regime of strong repulsive impurity-impurity interactions to which the case III belongs the concurrence is maximal, as implied by

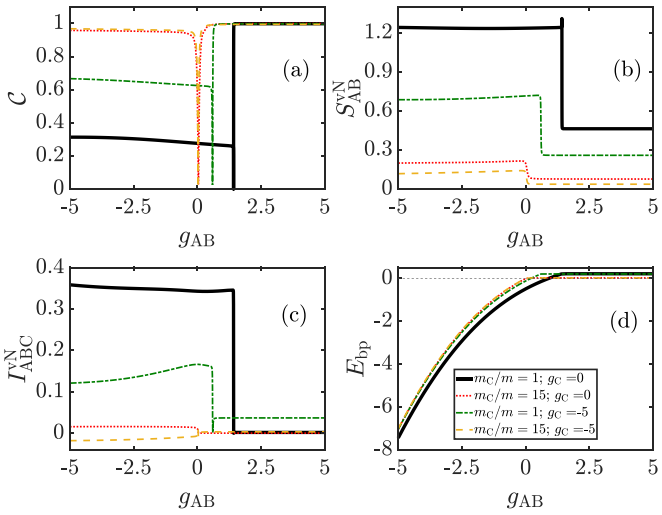

FIG. 3. The concurrence (a), the von Neumann entropy (b), the tripartite mutual information (c), and the bipolaron binding energy (d) as a function of the impurity-impurity interaction strength g_{AB} for $m_C/m = 1; g_C = 0$ (black line), $m_C/m = 15; g_C = 0$ (red line), $m_C/m = 1; g_C = -5$ (dark-green line), $m_C/m = 15; g_C = -5$ (yellow line). The dashed line in panel (d) indicates $E_{\mathrm{BP}} = 0$.

the populations of ρ_{LR} shown in Fig. 2(l), and signifies the appearance of the Bell state $|\Psi^+\rangle$ [44,51,52]. It is important to note that in this regime the von Neumann entropy is finite, taking values around $S^{\mathrm{vN}}_{AB} \approx 0.4$, indicating that the impurities are not entirely disconnected from the bosonic bath. Since the species C and the impurities are still entangled to some extent, this is another indicator that the bosonic matter-wave barrier which the impurities induce does exhibit quantum effects and cannot be considered equivalent to barriers formed by classical optical fields.

For decreasing impurity interaction g_{AB} there is a sudden transition in the concurrence as the impurities transition from being antibunched to being bunched. For mass-balanced systems (black lines in the following graphs) this transition is signaled by a narrow dip in the concurrence to zero in Fig. 3(a) and by a maximum in the von Neumann entropy S^{vN}_{AB} in Fig. 3(b), the latter reflecting increased correlations between the impurities and the bath. Both cases I and II lie to the left of this transition and take significantly lower values of the concurrence and also increased correlations with the bath. This implies that there is a tradeoff between the impurity-bath correlations and the impurity-impurity correlations, usually referred to as entanglement monogamy [53]. What is unclear is the stark difference between case I and III, with the latter possessing maximal concurrence while still having nonzero correlations with component C.

To understand this dichotomy we first note the differences in the structure of the bunched (cases I and II) and antibunched (case III) states. In the latter the impurities are spatially separated and therefore the probability to find both impurities and a bath particle at the same position is negligible. However, in the case of bunching such three-particle coincidences are more likely, therefore leading to the presence of three-body correlations, and we conjecture that these higher order correlations are responsible for the decoherence of the bipolaron

Bell state. To quantify the three-body correlations we compute the tripartite mutual information (TMI) [54]

$$I^{\mathrm{vN}}_{ABC} = I^{\mathrm{vN}}_{AC} + I^{\mathrm{vN}}_{BC} - I^{\mathrm{vN}}_{(AB)C}, \tag{6}$$

where $I^{\mathrm{vN}}_{\sigma\delta}$ is the mutual information between one σ-species particle and one δ-species particle defined as

$$I^{\mathrm{vN}}_{\sigma\delta} = S^{\mathrm{vN}}_{\sigma} + S^{\mathrm{vN}}_{\delta} - S^{\mathrm{vN}}_{\sigma\delta}, \tag{7}$$

while $I^{\mathrm{vN}}_{(AB)C}$ denotes the mutual information between the two impurities and one C-species boson:

$$I^{\mathrm{vN}}_{(AB)C} = S^{\mathrm{vN}}_{AB} + S^{\mathrm{vN}}_{C} - S^{\mathrm{vN}}_{ABC}. \tag{8}$$

Here S^{vN}_{σ} and $S^{\mathrm{vN}}_{\sigma\delta}$ are the respective single-particle and two-particle von Neumann entropies, while S^{vN}_{ABC} is the three-particle von Neumann entropy with one particle from each component A, B, and C. The tripartite mutual information is shown in Fig. 3(c), and as expected it vanishes when the impurities are antibunched, while it takes finite values when the impurities are bunched. This suggests that tripartite impurity-bath correlations are indeed responsible for decohering the $|\Phi^+\rangle$ state.

Finally, we note that the transition between bunching and antibunching occurs at finite values of $g_{AB} > 0$, as repulsive impurity-impurity interactions are required to counteract the mediated attractive interaction through the C component. The strength of these interactions can be quantified through the bipolaron binding energy [18]

$$E_{\mathrm{BP}} = E_2 - 2E_1 + E_0, \tag{9}$$

where E_2 is the ground-state energy of the total system with two impurities, E_1 denotes the ground-state energy of the system with one impurity, and E_0 is the energy of the system without any impurities. This is shown in Fig. 3(d), where the binding energy takes negative values when the impurities are bound together, notably occurring for zero impurity-impurity interaction at $g_{AB} = 0$. The transition between bunched and antibunched is signaled by the binding energy taking a constant value, occurring at the same value of g_{AB} as the major changes in the concurrence, the von Neumann entropy, and the mutual information. We note, however, that in the antibunched regime the binding energy does not vanish but instead takes a small but constant positive value, which is due to the finite size of the bath.

IV. IMPROVING IMPURITY-IMPURITY CORRELATIONS THROUGH ENVIRONMENT ENGINEERING

As we have shown, the coupling to the C component plays a crucial role in spatially separating the impurities from the bath and being able to create the impurity Bell states. On the other hand, the impurity-bath correlations that are created by this coupling also negatively affect the purity of the entangled impurity states and consequently cannot be completely separated from the bath. However, the properties of the bath are also tunable; for instance, by choosing a different atomic species the mass ratio m_C/m can be varied, while there is also some degree of control over the intraspecies interactions g_C. Let us first focus on adjusting the mass ratio while keeping $g_C = 0$ fixed. The von Neumann entropy, concurrence, mutual information, and binding energy are shown in Fig. 4 as a function of the mass ratio for fixed impurity-impurity interactions $g_{\mathrm{AB}} = -3, 0, 3$.

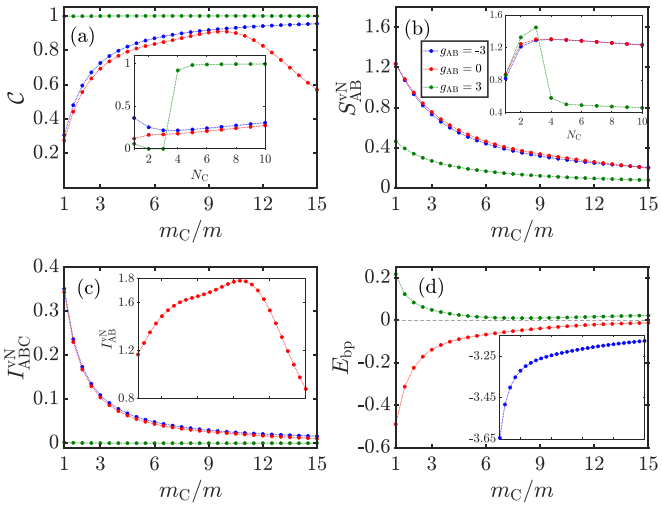

FIG. 4. Same as Fig. 3, but as a function of the mass ratio m_C/m for the impurity-impurity coupling strength $g_{AB} = -3$ (blue line), $g_{AB} = 0$ (red line), and $g_{AB} = 3$ (dark-green line). The insets in panel (a) and (b) show the concurrence $\mathcal{C}$ and the von Neumann entropy S^{vN}_{AB} as a function of N_C for the mass ratio $m_C/m = 1$, respectively. Meanwhile, the inset in panel (c) depicts the bipartite mutual information between two impurities as a function of the mass ratio for $g_{AB} = 0$. Note that the horizontal dashed line in panel (d) shows $E_{\mathrm{BP}} = 0$ and the x-axis range of insets in panels (c) and (d) is the same as that of the corresponding panels. In all panels, the bath is noninteracting, $g_C = 0$, and has $N_C = 10$ bosons.

It is immediately apparent from looking at the decay of the von Neumann entropy and tripartite mutual information that increasing the mass of the bath particles can significantly reduce the degree of the impurity-bath correlations. This can be well described by an algebraic decay of the form $S^{\mathrm{vN}}_{AB} \sim (m_C/m)^{-\alpha}$ and we show the fitted decay rates in Table I. It is worth mentioning that the decrease of the bath-mediated attractive interactions due to the larger mass of the bath particles compared to the impurities is in good agreement with the prediction in Ref. [21]. The same effect, albeit with a smaller decay rate, can be achieved by increasing the number of particles N_C, while keeping $m_C/m = 1$ [see inset of Fig. 4(b)], with the fits to $S^{\mathrm{vN}}_{AB} \sim N_C^{-\beta}$ shown again in Table I. It is evident that the exponent α is almost unaffected

TABLE I. Fitted exponents α and β. The number of bath particles used for fitting α is $N_C = 10$, while the mass ratio for fitting β is fixed at $m_C/m = 1$. To exclude any finite-size effects, we only consider values of $m_C/m \geqslant 2$ when determining α. Similarly, we use values of $6 \leqslant N_C \leqslant 10$ when determining β. In both cases the fitting equation is of the form $y = ax^{-r}$.

	$g_{\mathrm{AB}} = -3$	$g_{\mathrm{AB}} = 0$	$g_{\mathrm{AB}} = 3$
α	0.74	0.73	0.72
β	0.077	0.079	0.13

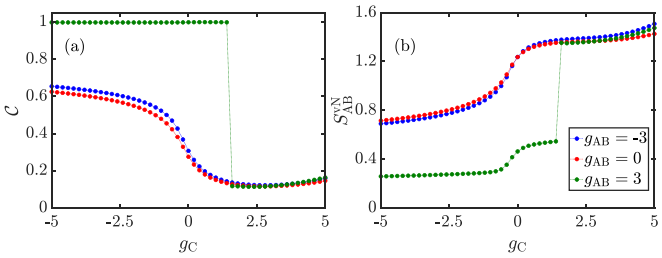

FIG. 5. The concurrence (a) and the von Neumann entropy (b) as a function of the intracomponent interaction strength g_C for $g_{AB} = -3$ (blue line), $g_{AB} = 0$ (red line), and $g_{AB} = 3$ (dark-green line). In all panels the mass ratio is $m_C/m = 1$.

by the interaction strength between the two impurities, while the decay rate β can be increased in the regime of repulsive impurity-impurity interactions. We also note that there is a minimum number of C particles that are needed to spatially separate the impurities, for instance $N_C > 3$ for $g_{AB} = 3$, as for smaller bath sizes the impurities are bunched in the center of the trap and hence the concurrence is roughly zero and the von Neumann entropy takes significantly larger values as shown in the insets in Figs. 4(a) and 4(b).

The enhancement of the correlations for the bunched states in case I can therefore be attributed to the screening of the bath-mediated interactions by the heavier mass of the bath which in turn reduces impurity-bath correlations and increases the coherence terms in ρ_{LR} [see Fig. 6(a)]. This screening effect may be quantified by a reduction in the bipolaron binding energy as shown in Fig. 4(d), and can be nicely understood by considering the special case of the bipolaron ($g_{AB} = 0$). In this case the impurities can only be correlated through the bath, therefore any impurity-impurity correlations are a byproduct of impurity-bath correlations. The decrease of the concurrence when $m_C > 10m$ is then a consequence of the reduction of the bath mediated interactions which are insufficient to tightly bind the impurities, leading to finite populations in $|\mathrm{LR}\rangle$ and $|\mathrm{RL}\rangle$. This decay can be further quantified by the bipartite mutual information $I_{AB} = S^{\mathrm{vN}}_A + S^{\mathrm{vN}}_B - S^{\mathrm{vN}}_{AB}$ [55,56] [see inset of Fig. 4(a)], which describes the continuous variable entanglement between the impurities. The mutual information similarly has to vanish when the impurities and bath become separable, and is therefore a more intuitive measure of the strength of the mediated attractive interactions in the system. We also highlight details of the screening effect of the increased mass ratio $m_C/m = 15$ in Fig. 3 (red dotted lines) as a function of g_{AB}. One can see that, when compared to the mass balanced case (black lines), the bunching to antibunching transition is shifted towards $g_{\mathrm{AB}} = 0$ as the bath mediated interactions are significantly diminished. Finally, in Fig. 5 we examine the effect of the bath intraspecies coupling strength, g_C, on the concurrence and von Neumann entropy for fixed $m_C = m$. Increasing the repulsive interactions between the C component atoms broadens the density distribution of the bath, and leads to an increase in the impurity-bath correlations due to larger wave-function overlap in the finite trap environment. This also adversely affects the concurrence for all the three cases we consider, with the sudden decrease for the case $g_{AB} = 3$ again a signal of this state transitioning from being antibunched to bunched. On the other hand, for attractive interactions $g_C < 0$ the concurrence is increased and the von Neumann entropy reduced, which indicates better conditions for the formation of the $|\Phi^+\rangle$ Bell state. Since the attractively interacting environment plays a role similar to the one of increasing mass, albeit to a lesser extent [see green dash-dotted lines in Fig. 3 and ρ_{LR} in Fig. 6(b)], a combination of both effects can be used to enhance the impurity-impurity correlations. To highlight this we show in Fig. 3 how bath interactions $g_C = -5$ in combination with a mass ratio of $m_C = 15m$ (yellow dashed lines) can be used to significantly improve the impurity-impurity correlations over the whole range of g_{AB}. Specifically, for $g_{AB} = -5$ the concurrence reaches $\mathcal{C} \approx 0.964$ while the von Neumann entropy is $S^{\mathrm{vN}}_{AB} \approx 0.125$. This characterizes a state that is close to the $|\Phi^+\rangle$ Bell state and we show ρ_{LR} for this case in Fig. 6(c). We also note that the TMI is negative for $g_{AB} < 0$, indicating that the composite system AB has more information compared to the individual systems A and B [54] due to it forming a tightly bound state.

It is also worth noting that the spatially antisymmetric Bell states, $|\Psi^-\rangle = (|\mathrm{LR}\rangle - |\mathrm{RL}\rangle)/\sqrt{2}$ and $|\Phi^-\rangle = (|\mathrm{LL}\rangle - |\mathrm{RR}\rangle)/\sqrt{2}$, naturally appear as the first excited states of the system. Although the OBDM and the diagonal TBDM of the first excited state are quite similar to those of the ground state due to the fact that they are nearly degenerate, we show in Fig. 7 that a clear difference appears in the reduced density matrix in the $\{|\mathrm{L}\rangle, |\mathrm{R}\rangle\}$ basis ρ_{LR} as the coherence terms are necessarily negative. Furthermore, we note that like the

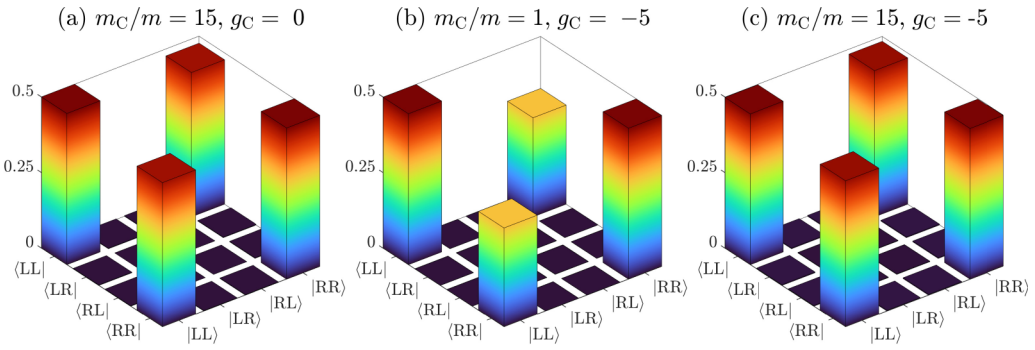

FIG. 6. The reduced density matrix ρ_{LR} for (a) $m_C/m = 15$, $g_C = 0$; (b) $m_C/m = 1$, $g_C = -5$; and (c) $m_C/m = 15$, $g_C = -5$. In all panels, the impurity-impurity coupling strength is $g_{AB} = -3$, and the bath has $N_C = 10$ bosons.

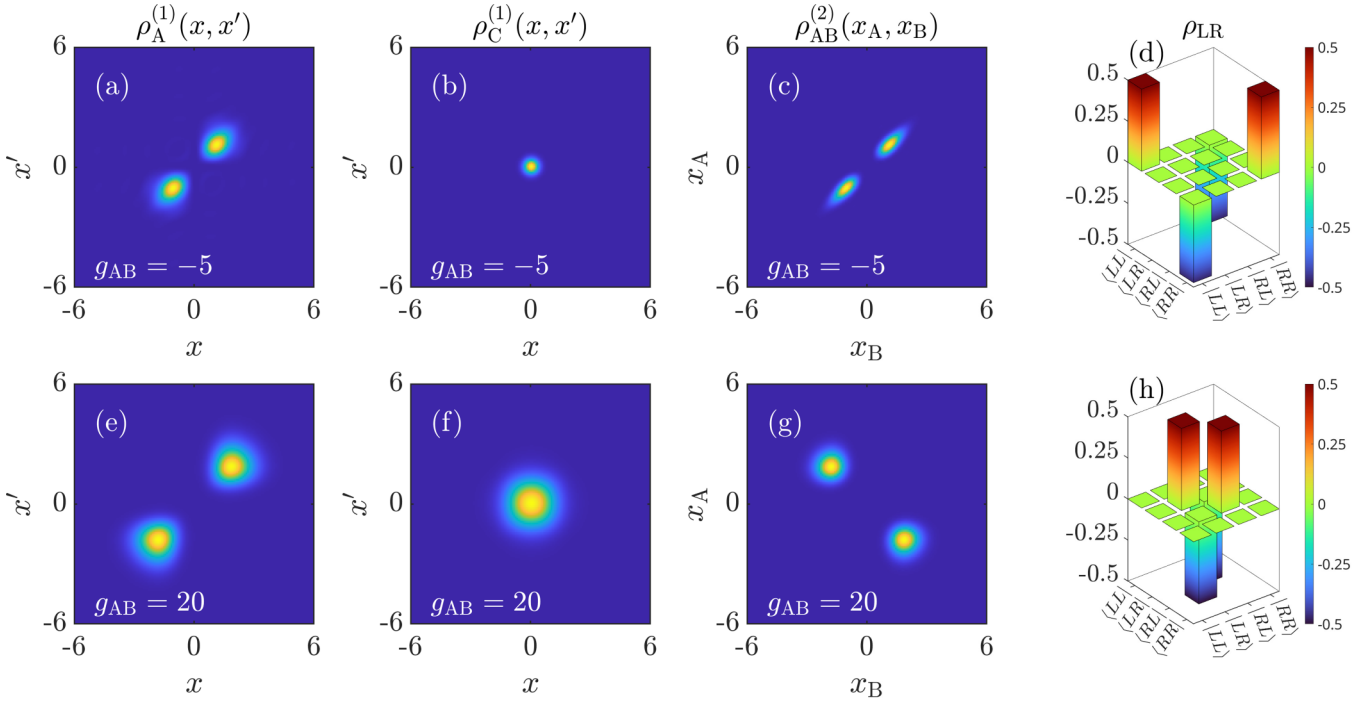

FIG. 7. The Bell states $|\Psi^-\rangle$ and $|\Phi^-\rangle$ are the first excited state of the corresponding system whose ground state demonstrates the states $|\Psi^+\rangle$ and $|\Phi^+\rangle$. The four columns are the OBDM $\rho_A^{(1)}(x,x')$, the OBDM $\rho_C^{(1)}(x,x')$, the diagonal TBDM $\rho_{AB}^{(2)}(x_A,x_B)=\rho_{AB}^{(2)}(x_A,x_B,x_A,x_B)$, and the reduced density matrix $\rho_{\rm LR}$, respectively. The different rows correspond to different cases, $g_{AB}=-5$, $m_C/m=15$ (upper row), and $g_{AB}=20$, $m_C/m=1$ (lower row). In all panels, the bosonic bath has $N_C=10$ noninteracting ($g_C=0$) bosons, while the impurity-bath coupling strengths are kept fixed, $g_{AC}=g_{BC}=5$. Note that all density matrices are normalized to unity.

spatially symmetric Bell states $|\Psi^+\rangle$ and $|\Phi^+\rangle$, we can also improve the fidelity of $|\Psi^-\rangle$ and $|\Phi^-\rangle$ by modifying the bath parameters such as its mass, giving us qualitatively similar results as discussed previously.

V. CONCLUSIONS

To summarize, we have proposed a scheme for robust preparation of strongly correlated states with current ultracold atomic setups, where particle numbers and interaction strengths are experimentally controllable, and where the spatial correlations we describe can be easily measured. We numerically demonstrate that strongly correlated states close to Bell states can be formed as ground states in systems of two distinguishable impurities immersed in a bosonic reservoir with a well-defined particle number. Our analysis shows that the Bell state $|\Psi^+\rangle$ can be readily generated with two repulsively interacting impurities, while the Bell state $|\Phi^+\rangle$ is hard to achieve due to large correlations created between the bath and impurities which reduce the state coherence. With the aim of reducing the impact of impurity-bath correlations such that the entanglement between the two impurities can be further enhanced, we have investigated the properties of the bath including its intraspecies coupling strength, and the mass of its particles. We have demonstrated that in both situations the formation of the Bell states is substantially enhanced compared to the mass-balanced noninteracting bath. Importantly, we have shown in this paper that the bosonic bath located in the center of the harmonic trap forms a matter barrier to separate the two impurities resulting in the emergence of their nonclassical properties. We emphasize that this effect is a purely quantum phenomenon proven by the finite von Neumann entropy between the bosonic bath and impurities and that it is significantly different from classical potentials. We anticipate that our results not only pave an efficient and experimentally feasible way to create and fully control strongly correlated atomic states, but also will stimulate further research on the nonclassical properties of multicomponent quantum systems.

ACKNOWLEDGMENTS

The authors thank M. Boubakour and N. Harshman for enlightening discussions. This work is supported by the Okinawa Institute of Science and Technology Graduate University (OIST). The numerical calculations were performed on the computational resources provided by the Scientific Computing and Data Analysis section at OIST. T.F., T.B., and T.D.A.-T. are grateful to Japan Science and Technology Agency Grant No. JPMJPF2221 and T.F. also acknowledges support from Japan Society for the Promotion of Science KAKENHI Grant No. JP23K03290. T.D.A.-T. expresses his gratitude to the Pure and Applied Mathematics University Research Institute at the Polytechnic University of Valencia for their hospitality to M.A.G.-M. during his visit. M.A.G.-M. acknowledges support from the Ministry for Digital Transformation and Civil Service of the Spanish Government through the QUANTUM ENIA Quantum Spain project, and by the European Union through the Recovery, Transformation, and Resilience Plan—NextGenerationEU within the

framework of the Digital Spain 2026 Agenda, as well as from Projects of MCIN with funding from European Union NextGenerationEU (Grant No. PRTR-C17.I1) and by Generalitat Valenciana (PerovsQuTe Grant No. 20220883) and QuanTwin Grant No. COMCUANTICA/007, and Red Tematica Grant No. RED2022-134391-T.

APPENDIX A: NUMERICAL METHOD

In the following, we briefly summary the *ab initio* method used in this paper, the improved exact diagonalization method [43]. For numerical purposes, it is naturally convenient to diagonalize the many-body Hamiltonian in the formalism of second quantization. In doing so, the field operators are introduced as

$$\hat{\Psi}_\sigma(x) = \sum_k \phi_{\sigma,k}(x)\hat{a}_{\sigma,k}, \tag{A1}$$

$$\hat{\Psi}^\dagger_\sigma(x) = \sum_k \phi^*_{\sigma,k}(x)\hat{a}^\dagger_{\sigma,k}. \tag{A2}$$

The field operator $\hat{\Psi}_\sigma(x)$ ($\hat{\Psi}^\dagger_\sigma(x)$) annihilates (creates) a σ-species boson being in the single-particle state $\phi_{\sigma,k}(x)$ at position x. Here $\hat{a}_{\sigma,k}$ ($\hat{a}^\dagger_{\sigma,k}$) corresponds to the annihilation (creation) operator. For bosonic systems, the creation and annihilation operators must obey the commutation relations

$$[\hat{a}_{\sigma,k}, \hat{a}^\dagger_{\delta,\ell}] = \delta_{\sigma\delta}\delta_{k\ell}, \tag{A3}$$

$$[\hat{a}^\dagger_{\sigma,k}, \hat{a}^\dagger_{\delta,\ell}] = [\hat{a}_{\sigma,k}, \hat{a}_{\delta,\ell}] = 0. \tag{A4}$$

The resulting Hamiltonian is then given as

$$\hat{H} = \sum_{\sigma\in\{A,B,C\}} \sum_{k,\ell} h^\sigma_{k\ell}\hat{a}^\dagger_{\sigma,k}\hat{a}_{\sigma,\ell} + \frac{1}{2}\sum_{k\ell mn} W^C_{k\ell mn}\hat{a}^\dagger_{C,k}\hat{a}^\dagger_{C,\ell}\hat{a}_{C,m}\hat{a}_{C,n} + \sum_{\sigma\neq\delta\in\{A,B,C\}} \sum_{k\ell mn} W^{\sigma\delta}_{k\ell mn}\hat{a}^\dagger_{\sigma,k}\hat{a}^\dagger_{\delta,\ell}\hat{a}_{\sigma,m}\hat{a}_{\delta,n}. \tag{A5}$$

Here $h^\sigma_{k\ell}$, $W^C_{k\ell mn}$, and $W^{\sigma\delta}_{k\ell mn}$ are one- and two-body matrix elements expressed in the basis of the single-particle Hamiltonian. As the system we consider is confined in a 1D harmonic trap, it is straightforward to employ the harmonic oscillator eigenfunctions as the single-particle functions $\phi_{\sigma,k}(x)$. This choice makes use of analytical results to obtain the matrix elements $h^\sigma_{k\ell} = (k+0.5)\delta_{k\ell}$, $W^C_{k\ell mn}$, and $W^{\sigma\delta}_{k\ell mn}$, thus the convergence is accelerated. Further details of this approach can be found in Refs. [43,57–60].

The ansatz wave function is factorized as a linear combination of a set of orthonormal Fock states

$$|\Psi\rangle = \sum_{j_A=1}^{D_A}\sum_{j_B=1}^{D_B}\sum_{j_C=1}^{D_C} c_{j_A,j_B,j_C}\left|\Phi^A_{j_A}\right\rangle\left|\Phi^B_{j_B}\right\rangle\left|\Phi^C_{j_C}\right\rangle. \tag{A6}$$

Here, c_{j_A,j_B,j_C} denote the expansion coefficients and $|\Phi^\sigma_{j_\sigma}\rangle = |n^\sigma_1, n^\sigma_2 \ldots n^\sigma_k \ldots\rangle$ is a possible σ-species permanent (also known as configuration) in the total of D_σ permanents used to expand the ansatz. Note that in each permanent, the occupation number n^σ_k in the single-particle state $\phi_{\sigma,k}(x)$ can be arbitrary integers between zero and N_σ and must obey the constraint $\sum_k n^\sigma_k = N_\sigma$. In practice, the permanents for the ansatz are selected such that their energies in the noninteracting many-body Hamiltonian are less than a certain optimal value $E_{\max}$. This truncation approach is known as the energy-cutoff scheme proposed in Refs. [61,62] and hence the accuracy of the numerical results is controlled by increasing $E_{\max}$. The key ingredient of the improved exact diagonalization scheme which significantly reduces the number of required permanents is the selection of dominant configurations in terms of the spatial symmetry of the desired many-body state [43]. It is known that if the trapping potential of a quantum particle has a spatial symmetry, namely,

$$V(x) = V(-x), \tag{A7}$$

then the single-particle eigenfunctions $\phi_k(x)$ possess a well-defined spatial symmetry. Mathematically, the spatially symmetric $\phi_{k=2n}(x)$ are even functions, while the spatially asymmetric $\phi_{k=2n+1}(x)$ are odd functions. Because the permanents are the symmetrized Hartree product of the single-particle functions $\phi_k(x)$, they must satisfy this spatial symmetry. This leads to the fact that the desired wave functions are solely expanded by either even- or odd-parity permanents. Thus, it is more practical to use only the permanents that have the same parity as the desired many-body wave function in the expansion of the ansatz. Since the bosonic ground-state wave function is spatially symmetric, we therefore only use even-parity permanents for the ansatz in this paper. Meanwhile, for obtaining the first excited state, the ansatz is expanded by odd-parity permanents.

In general, minimizing the expectation value of the Hamiltonian (A5) with respect to the ansatz (A6) leads to the standard Hermitian eigenvalue problem which can be written in the form of

$$\mathbf{H}|C_m\rangle = E_m|C_m\rangle, \tag{A8}$$

with $\mathbf{H}$ being the matrix representation of the many-body Hamiltonian (A5). The pair $\{E_m, |C_m\rangle\}$ is the mth many-body eigenvalue and eigenvector, respectively.

[1] A. Acín, I. Bloch, H. Buhrman, T. Calarco, C. Eichler, J. Eisert, D. Esteve, N. Gisin, S. J. Glaser, F. Jelezko, S. Kuhr, M. Lewenstein, M. F. Riedel, P. O. Schmidt, R. Thew, A. Wallraff, I. Walmsley, and F. K. Wilhelm, The quantum technologies roadmap: A European community view, New J. Phys. **20**, 080201 (2018).

[2] J. Eisert, D. Hangleiter, N. Walk, I. Roth, D. Markham, R. Parekh, U. Chabaud, and E. Kashefi, Quantum certification and benchmarking, Nat. Rev. Phys. **2**, 382 (2020).

[3] J. Fraxanet, T. Salamon, and M. Lewenstein, The coming decades of quantum simulation, in *Sketches of Physics: The Celebration Collection*, edited by R. Citro, M. Lewenstein, A.

Rubio, W. P. Schleich, J. D. Wells, and G. P. Zank (Springer, New York, 2023), pp. 85–125.

[4] R. Horodecki, P. Horodecki, M. Horodecki, and K. Horodecki, Quantum entanglement, Rev. Mod. Phys. **81**, 865 (2009).

[5] N. Brunner, D. Cavalcanti, S. Pironio, V. Scarani, and S. Wehner, Bell nonlocality, Rev. Mod. Phys. **86**, 419 (2014).

[6] S. Mistakidis, A. Volosniev, R. Barfknecht, T. Fogarty, T. Busch, A. Foerster, P. Schmelcher, and N. Zinner, Few-body Bose gases in low dimensions: A laboratory for quantum dynamics, Phys. Rep. **1042**, 1 (2023).

[7] T. Sowiński and M. Á. García-March, One-dimensional mixtures of several ultracold atoms: A review, Rep. Prog. Phys. **82**, 104401 (2019).

[8] A. Schirotzek, C.-H. Wu, A. Sommer, and M. W. Zwierlein, Observation of Fermi polarons in a tunable Fermi liquid of ultracold atoms, Phys. Rev. Lett. **102**, 230402 (2009).

[9] P. Massignan, M. Zaccanti, and G. M. Bruun, Polarons, dressed molecules and itinerant ferromagnetism in ultracold Fermi gases, Rep. Prog. Phys. **77**, 034401 (2014).

[10] N. B. Jørgensen, L. Wacker, K. T. Skalmstang, M. M. Parish, J. Levinsen, R. S. Christensen, G. M. Bruun, and J. J. Arlt, Observation of attractive and repulsive polarons in a Bose-Einstein condensate, Phys. Rev. Lett. **117**, 055302 (2016).

[11] M.-G. Hu, M. J. Van de Graaff, D. Kedar, J. P. Corson, E. A. Cornell, and D. S. Jin, Bose polarons in the strongly interacting regime, Phys. Rev. Lett. **117**, 055301 (2016).

[12] R. Schmidt, M. Knap, D. A. Ivanov, J.-S. You, M. Cetina, and E. Demler, Universal many-body response of heavy impurities coupled to a Fermi sea: A review of recent progress, Rep. Prog. Phys. **81**, 024401 (2018).

[13] C. Baroni, B. Huang, I. Fritsche, E. Dobler, G. Anich, E. Kirilov, R. Grimm, M. A. Bastarrachea-Magnani, P. Massignan, and G. M. Bruun, Mediated interactions between Fermi polarons and the role of impurity quantum statistics, Nat. Phys. **20**, 68 (2024).

[14] M. Cetina, M. Jag, R. S. Lous, I. Fritsche, J. T. Walraven, R. Grimm, J. Levinsen, M. M. Parish, R. Schmidt, M. Knap *et al.*, Ultrafast many-body interferometry of impurities coupled to a Fermi sea, Science **354**, 96 (2016).

[15] M. Cetina, M. Jag, R. S. Lous, J. T. M. Walraven, R. Grimm, R. S. Christensen, and G. M. Bruun, Decoherence of impurities in a Fermi sea of ultracold atoms, Phys. Rev. Lett. **115**, 135302 (2015).

[16] A. Lampo, S. H. Lim, M. Á. García-March, and M. Lewenstein, Bose polaron as an instance of quantum brownian motion, Quantum **1**, 30 (2017).

[17] L. D. Landau and S. I. Pekar, 67 - The effective mass of the polaron, J.Exp.Theor.Phys. **18**, 419 (1948).

[18] A. Camacho-Guardian, L. A. P. Ardila, T. Pohl, and G. M. Bruun, Bipolarons in a Bose-Einstein condensate, Phys. Rev. Lett. **121**, 013401 (2018).

[19] C. Charalambous, M. A. Garcia-March, A. Lampo, M. Mehboud, and M. Lewenstein, Two distinguishable impurities in BEC: Squeezing and entanglement of two Bose polarons, SciPost Phys. **6**, 010 (2019).

[20] W. Casteels, J. Tempere, and J. T. Devreese, Bipolarons and multipolarons consisting of impurity atoms in a Bose-Einstein condensate, Phys. Rev. A **88**, 013613 (2013).

[21] A. Camacho-Guardian and G. M. Bruun, Landau effective interaction between quasiparticles in a Bose-Einstein condensate, Phys. Rev. X **8**, 031042 (2018).

[22] M. Will, G. E. Astrakharchik, and M. Fleischhauer, Polaron interactions and bipolarons in one-dimensional Bose gases in the strong coupling regime, Phys. Rev. Lett. **127**, 103401 (2021).

[23] J. Jager and R. Barnett, The effect of boson-boson interaction on the bipolaron formation, New J. Phys. **24**, 103032 (2022).

[24] J. Tempere, W. Casteels, M. K. Oberthaler, S. Knoop, E. Timmermans, and J. T. Devreese, Feynman path-integral treatment of the BEC-impurity polaron, Phys. Rev. B **80**, 184504 (2009).

[25] B. Kain and H. Y. Ling, Polarons in a dipolar condensate, Phys. Rev. A **89**, 023612 (2014).

[26] B. Kain and H. Y. Ling, Generalized Hartree-Fock-Bogoliubov description of the Fröhlich polaron, Phys. Rev. A **94**, 013621 (2016).

[27] F. Grusdt, All-coupling theory for the Fröhlich polaron, Phys. Rev. B **93**, 144302 (2016).

[28] F. Grusdt, G. E. Astrakharchik, and E. Demler, Bose polarons in ultracold atoms in one dimension: beyond the Fröhlich paradigm, New J. Phys. **19**, 103035 (2017).

[29] M. Drescher, M. Salmhofer, and T. Enss, Medium-induced interaction between impurities in a Bose-Einstein condensate, Phys. Rev. A **107**, 063301 (2023).

[30] R. Schmidt and T. Enss, Self-stabilized Bose polarons, SciPost Phys. **13**, 054 (2022).

[31] A. Petković and Z. Ristivojevic, Mediated interaction between polarons in a one-dimensional Bose gas, Phys. Rev. A **105**, L021303 (2022).

[32] M. Mehboudi, A. Lampo, C. Charalambous, L. A. Correa, M. Á. García-March, and M. Lewenstein, Using polarons for sub-nk quantum nondemolition thermometry in a Bose-Einstein condensate, Phys. Rev. Lett. **122**, 030403 (2019).

[33] A. Lampo, C. Charalambous, M. Á. García-March, and M. Lewenstein, Non-Markovian polaron dynamics in a trapped Bose-Einstein condensate, Phys. Rev. A **98**, 063630 (2018).

[34] M. M. Khan, H. Terças, J. T. Mendonça, J. Wehr, C. Charalambous, M. Lewenstein, and M. A. García-March, Quantum dynamics of a Bose polaron in a *d*-dimensional Bose-Einstein condensate, Phys. Rev. A **103**, 023303 (2021).

[35] D. Breu, E. V. Marcos, M. Will, and M. Fleischhauer, Impurities in a trapped 1D Bose gas of arbitrary interaction strength: Localization-delocalization transition and absence of self-localization, arXiv:2408.11549.

[36] L. Zschetzsche and R. E. Zillich, Suppression of polaron self-localization by correlations, Phys. Rev. Res. **6**, 023137 (2024).

[37] M. García-March, A. S. Dehkharghani, and N. Zinner, Entanglement of an impurity in a few-body one-dimensional ideal Bose system, J. Phys. B **49**, 075303 (2016).

[38] A. S. Dehkharghani, A. G. Volosniev, and N. T. Zinner, Coalescence of two impurities in a trapped one-dimensional Bose gas, Phys. Rev. Lett. **121**, 080405 (2018).

[39] K. Keiler, S. I. Mistakidis, and P. Schmelcher, Polarons and their induced interactions in highly imbalanced triple mixtures, Phys. Rev. A **104**, L031301 (2021).

[40] F. Theel, S. I. Mistakidis, K. Keiler, and P. Schmelcher, Counterflow dynamics of two correlated impurities immersed in a bosonic gas, Phys. Rev. A **105**, 053314 (2022).

[41] S. I. Mistakidis, A. G. Volosniev, and P. Schmelcher, Induced correlations between impurities in a one-dimensional quenched Bose gas, Phys. Rev. Res. **2**, 023154 (2020).

[42] F. Theel, S. I. Mistakidis, and P. Schmelcher, Crossover from attractive to repulsive induced interactions and bound states of two distinguishable Bose polarons, SciPost Phys. **16**, 023 (2024).

[43] T. D. Anh-Tai, M. Mikkelsen, T. Busch, and T. Fogarty, Quantum chaos in interacting Bose-Bose mixtures, SciPost Phys. **15**, 048 (2023).

[44] A. Bergschneider, V. M. Klinkhamer, J. H. Becher, R. Klemt, L. Palm, G. Zürn, S. Jochim, and P. M. Preiss, Experimental characterization of two-particle entanglement through position and momentum correlations, Nat. Phys. **15**, 640 (2019).

[45] K. Huang and C. N. Yang, Quantum-mechanical many-body problem with hard-sphere interaction, Phys. Rev. **105**, 767 (1957).

[46] C. Chin, R. Grimm, P. Julienne, and E. Tiesinga, Feshbach resonances in ultracold gases, Rev. Mod. Phys. **82**, 1225 (2010).

[47] E. Haller, M. J. Mark, R. Hart, J. G. Danzl, L. Reichsöllner, V. Melezhik, P. Schmelcher, and H.-C. Nägerl, Confinement-induced resonances in low-dimensional quantum systems, Phys. Rev. Lett. **104**, 153203 (2010).

[48] M. Olshanii, Atomic scattering in the presence of an external confinement and a gas of impenetrable bosons, Phys. Rev. Lett. **81**, 938 (1998).

[49] M. Taglieber, A.-C. Voigt, T. Aoki, T. W. Hänsch, and K. Dieckmann, Quantum degenerate two-species Fermi-Fermi mixture coexisting with a Bose-Einstein condensate, Phys. Rev. Lett. **100**, 010401 (2008).

[50] C.-H. Wu, I. Santiago, J. W. Park, P. Ahmadi, and M. W. Zwierlein, Strongly interacting isotopic Bose-Fermi mixture immersed in a Fermi sea, Phys. Rev. A **84**, 011601(R) (2011).

[51] M. Bonneau, W. J. Munro, K. Nemoto, and J. Schmiedmayer, Characterizing twin-particle entanglement in double-well potentials, Phys. Rev. A **98**, 033608 (2018).

[52] A. Usui, T. Fogarty, S. Campbell, S. A. Gardiner, and T. Busch, Spin–orbit coupling in the presence of strong atomic correlations, New J. Phys. **22**, 013050 (2020).

[53] V. Coffman, J. Kundu, and W. K. Wootters, Distributed entanglement, Phys. Rev. A **61**, 052306 (2000).

[54] A. Seshadri, V. Madhok, and A. Lakshminarayan, Tripartite mutual information, entanglement, and scrambling in permutation symmetric systems with an application to quantum chaos, Phys. Rev. E **98**, 052205 (2018).

[55] G. Bellomia, C. Mejuto-Zaera, M. Capone, and A. Amaricci, Quasilocal entanglement across the Mott-Hubbard transition, Phys. Rev. B **109**, 115104 (2024).

[56] L. Amico, R. Fazio, A. Osterloh, and V. Vedral, Entanglement in many-body systems, Rev. Mod. Phys. **80**, 517 (2008).

[57] J. Rotureau, Interaction for the trapped Fermi gas from a unitary transformation of the exact two-body spectrum, Eur. Phys. J. D **67**, 153 (2013).

[58] E. Lindgren, J. Rotureau, C. Forssén, A. G. Volosniev, and N. T. Zinner, Fermionization of two-component few-fermion systems in a one-dimensional harmonic trap, New J. Phys. **16**, 063003 (2014).

[59] A. Dehkharghani, A. Volosniev, J. Lindgren, J. Rotureau, C. Forssén, D. Fedorov, A. Jensen, and N. Zinner, Quantum magnetism in strongly interacting one-dimensional spinor Bose systems, Sci. Rep. **5**, 10675 (2015).

[60] L. Rammelmüller, D. Huber, and A. G. Volosniev, A modular implementation of an effective interaction approach for harmonically trapped fermions in 1D, SciPost Phys. Codebases, 12 (2023).

[61] A. Chrostowski and T. Sowinski, Efficient construction of many-body Fock states having the lowest energies, Acta Phys. Pol. A **136**, 566 (2019).

[62] M. Plodzien, D. Wiater, A. Chrostowski, and T. Sowinski, Numerically exact approach to few-body problems far from a perturbative regime, arXiv:1803.08387.